

# **Extract Object Boundaries in Noisy Images using Level Set**

**by: Quming Zhou**

## **Final Report**

Submitted to Professor Brian Evans

EE381K Multidimensional Digital Signal Processing

May 10, 2003

### **Abstract**

Finding object contours in noisy images is a challenging task because of the amorphous nature of the object and the lack of sharp boundaries. Classical edge-based segmentation methods have the drawback of not connecting edge segments to form a distinct and meaningful boundary. Many level set approaches, which can deal with changes of topology and the presence of corners, have been developed to extract object boundaries. Previous researchers have used image gradient, edge strength, area minimization and region intensity to define the speed function. However, no paper mentions the edge/gradient direction. Our approach will incorporate direction and magnitude in the speed function.

## 1. Introduction

Many computer vision applications involve the decomposition of image into regions with homogeneous properties, which are related to the nature of the application. The boundary of an object is an important feature for the object detection, classification and tracking. Edge based approaches are not suitable for boundary extraction in noisy images [1]. They will detect edges that are not part of an object's boundary or miss parts of a boundary when the intensity contrast is weak. In general, additional effort is needed to connect the incomplete edges into a distinct and meaningful object boundary.

Several approaches have been proposed to extract object boundaries in images using closed curves. Roughly speaking, there are two types of boundary search approaches. One uses a closed contour represented by a parameterized curve. The problem of finding the desirable contour is posed as an energy minimization problem. The classical Euler-Lagrange formulation of the active contour is called 'snake' [2]. This kind of method relies on an initial guess of the boundary, image features and parameters. Moreover, its performance suffers from the change of topology and the presence of corners.

To overcome these problems, the level set approach has been proposed [3]. The guiding principle of level set methods is to describe a closed curve  $\gamma$  in  $R^2$  as the zero level set of a higher dimensional function  $\Phi(x, y, t)$  in  $R^3$ . Instead of propagating the curve  $\gamma$  directly, we consider the evolution of function  $\Phi(x, y, t)$  with a speed function  $F$  and extract the zero level set of points to obtain the boundary curve. Since level set methods represent the curve in an implicit form, they greatly simplify the management of the contour evolution, especially for handling topological changes. Most of the challenges in level set methods result from the need to construct an adequate model for the speed function.

## 2. Background

We consider the generation of a family of contours. Let an initial curve  $r_0$  undergo deformation in a Euclidean plane. Let  $r(x, y, t)$  denote the family of curves generated by the propagation of  $r_0$  in the outward normal direction  $\vec{N}$  with the speed  $F$ . We ignore the tangential velocity because it does not influence the geometry of the deformation, but only its parameterization [4]. The curve velocity  $r_t(x, y, t)$  is denoted by

$$r_t(x, y, t) = F\vec{N}, \quad (1)$$

where  $F$  is a scalar function and  $\vec{N}$  is a unit normal vector.

According to the level set method, we can express the closed curve  $r(t)$  in an implicit form as

$$r(x, y, t) = \{(x, y) | \Phi(x, y, t) = 0\}, \text{ or } \Phi(r(t), t) = 0. \quad (2)$$

By the chain rule,

$$\Phi_t + \Phi_r \cdot r_t = \Phi_t + \nabla\Phi \cdot F\vec{N} = \Phi_t + \nabla\Phi \cdot F \frac{\nabla\Phi}{|\nabla\Phi|} = 0,$$

yielding the movement equation of curves,

$$\Phi_t + F|\nabla\Phi| = 0, \text{ with } \Phi(x, y, t = 0) = r_0. \quad (3)$$

The speed function is essentially a decreasing function of a set of features. These features should have very high values at the final shape boundary. In general, speed function models can be classified as edge-based and region-based.

## 2.1 Speed Function Due to Image Gradient

Caselle *et al.* [5] proposed the geometric active contour followed by Malladi *et al.* [6]. The model proposed by Caselle and Malladi was based on the following speed function:

$$F = (a + \varepsilon k) / |1 + \nabla G_\sigma * I|, \quad (4)$$

where  $k$  is the curvature of the curve,  $a$ ,  $\varepsilon$  and  $p$  are constants and  $|1 + \nabla G_\sigma * I|$  is the edge gradient using a Gaussian filter  $G_\sigma$  with a known standard deviation  $\sigma$ . Since the stop criterion is the magnitude of the gradient, the speed slows down at strong edges. The drawback of this model is that it only detects objects with edges defined by strong gradients.  $F$  is never small enough to stop the curve evolution in a noisy image and the curve may extend beyond the boundary. Moreover the pulling back force is not strong hence it may not be able to pull back the expanding contour if it were to propagate and cross the desired boundary.

## 2.2 Speed Function Due to Region Intensity

Chan *et al.* [7] proposed an active model based on Mumford-Shan segmentation technique and the level set method. Their model can extract objects whose boundaries are not necessarily defined by gradient or with very smooth boundaries. They introduced the energy function  $F(c_1, c_2, C)$ , defined by

$$F(c_1, c_2, C) = u \cdot \text{Length}(C) + v \cdot \text{Area}(\text{inside}(C)) + \lambda_1 \int_{\text{inside}(C)} |u_0(x, y) - c_1|^2 dx dy + \lambda_2 \int_{\text{outside}(C)} |u_0(x, y) - c_2|^2 dx dy \quad (5)$$

where  $u \geq 0, v \geq 0, \lambda_1, \lambda_2 > 0$  are fixed parameters,  $u_0(x, y)$  is the intensity of pixel  $(x, y)$ ,  $C$  is the curve, while the constants  $c_1$  and  $c_2$  depending on  $C$ , are the average of  $u_0$  inside or outside the

curve  $C$ . Finding the object boundary turns out to be the minimization of the energy  $F(c_1, c_2, C)$ . For the level set formulation of the variation active contour model, they deduced the associate Euler-Lagrange equation for  $\Phi$  as

$$\begin{aligned} \frac{\partial \Phi}{\partial t} &= \delta_\varepsilon(\Phi) [u \cdot \text{div}(\frac{\nabla \Phi}{|\nabla \Phi|}) - v - \lambda_1 (u_0 - c_1)^2 + \lambda_2 (u_0 - c_2)^2] = 0 \text{ in } (0, \infty) \times \Omega, \\ \Phi(0, x, y) &= \Phi_0(x, y) \text{ in } \Omega, \quad \frac{\delta_\varepsilon(\Phi)}{|\nabla \Phi|} \frac{\partial \Phi}{\partial \bar{n}} = 0 \text{ on } \partial \Omega \end{aligned} \quad (6)$$

where  $\bar{n}$  denotes the exterior normal to the boundary  $\partial \Omega$ ,  $\partial \Phi / \partial \bar{n}$  denotes the normal derivation of  $\Phi$  at the boundary, and  $\delta_\varepsilon(\Phi)$  is the regulation function.

The problem with this method is that we have to estimate the intensity distribution of the region; however, the distribution model may degrade in a noisy image.

### 3: The Proposed Method

The proposed approach uses the edge direction as well as the gradient magnitude. A strong edge can stop the curve evolution by its gradient magnitude. A weak edge can halt the curve by its edge map direction, which points toward the closest boundary. The result of evolution will be a curve that goes through the most homogenous region to fit the object boundary. When the speed function is small, the evolution process ceases.

#### 3.1 Edge Map

The motivation for the edge map comes from the fact that the magnitude of the intensity gradient cannot restrict the level set flow completely and the edge direction will help us localize the edge. We introduce a concept, edge map, to represent the gradient magnitude and direction. Edge flow detects the image boundaries by identifying the location, which has non-zero edge flow coming from two opposite directions. We explore the isotropic and linear characteristics of Gaussian filters to obtain the edge map, which accounts for the local edge gradients and their neighborhood.

A 2D isotropic Gaussian filter with standard deviation  $\sigma$  is applied to the image  $I(x, y)$ . The smoothed image is denoted by  $I_\sigma(x, y)$ . Further, the gradient images  $g_x(x, y)$  and  $g_y(x, y)$  are computed by the first order difference of  $I_\sigma(x, y)$  along x-axis and y-axis respectively. Then, the local edge vector at pixel  $s = (x_s, y_s)$  along the orientation  $\theta$  is a linear combination as

$$\vec{E}(s, \theta) = (g_x(s) \cos(\theta) + g_y(s) \sin(\theta)) \angle \theta. \quad (7)$$

where  $g_x(s)$  and  $g_y(s)$  are the gradients, for pixel  $s$ , along the x-axis and y-axis respectively.

$\vec{E}(s, \theta)$  is the local edge vector along the orientation  $\theta$ . It gives us the local intensity change, which is widely used in edge detectors. Our edge map for pixel  $s$  is defined by

$$\vec{M}(s) = \int_{\theta'}^{\theta'+\pi} \vec{E}(s, \theta) d\theta. \quad (8)$$

The integration range parameter  $\theta'$  is now estimated. Without loss of generality, for the pixel  $s = (x_s, y_s)$ , we compute the intensity difference with pixel  $s' = (x_s + d \cos \theta, y_s + d \sin \theta)$  as

$$Diff(s, \theta) = |I_\sigma(x_s + d \cos \theta, y_s + d \sin \theta) - I_\sigma(x_s, y_s)|, \quad (9)$$

where  $d = 5\sigma$ . We assume that  $Diff(s, \theta)$  is usually no less than  $Diff(s, \theta + \pi)$  when the boundary is a distance  $d$  away from the pixel  $s$  in the direction  $\theta$ . However it is still not enough to know where the boundary is exactly. To quantify the prediction of the boundary, an index  $P(s, \theta)$  is assigned to every pixel with the same offset distance,  $d$ , from the pixel  $s$  by

$$P(s, \theta) = \frac{Diff(s, \theta) - Diff(s, \theta + \pi)}{Diff(s, \theta) + Diff(s, \theta + \pi)}. \quad (10)$$

A large index value implies a boundary located in that direction. We choose  $\theta'$  in order to maximize the integration of  $P(s, \theta)$  in the corresponding half plane:

$$\theta' = \arg \max_{\theta'} \int_{\theta'}^{\theta'+\pi} P(s, \theta) d\theta. \quad (11)$$

The edge map  $\vec{M}(s)$  is a vector pointing toward the closest boundary pixel with its magnitude representing the total gradient energy in the half plane. Figure 1 shows an example of the edge map for  $\sigma = 1$ . Each arrow indicates the magnitude and the direction of a pixel. The cycle points are the edge pixels obtained by the Canny edge detector. As we can see, the direction of the edge map points to its nearest boundary as its magnitude varies with the distance from the boundary.

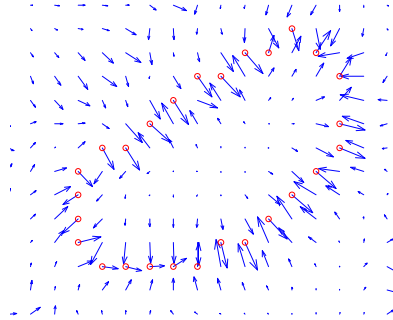


Fig. 1. Edge map for each pixel.

### 3.2 Speed Function

We define our speed function in the outward normal direction of the curve as

$$F = (c - \varepsilon k) / g(\vec{M}), \quad (12)$$

where  $c$  and  $\varepsilon$  are constants,  $k$  is the curvature and  $g(\vec{M})$  is a scaling function of the edge map  $\vec{M}$ . Physically,  $c$  denotes an expansion term,  $\varepsilon k$  plays the smoothing role and  $g(\vec{M})$  is a stop criterion. The value of  $g(\vec{M})$  depends on the magnitude of the edge map as well as its direction. We give its formula as follows.

Let  $\theta$  be the angle between the edge map and the outward normal vector  $\vec{N}$ . Then,

$$g(\vec{M}) = \begin{cases} 1 + |\vec{M}| & \text{if } \cos\theta \geq 0 \\ 1 + |\vec{M}|^2 & \text{if } -0.5 \leq \cos\theta < 0 \\ 1 + (3 \sim 5) |\vec{M}|^2 & \text{otherwise} \end{cases}$$

The ability to slow down the speed function varies with the direction of the edge map. An edge map with a low magnitude value in the direction opposite to the outward curve normal direction will have a halting ability comparable to that of the strong edge map. Thus, the speed function has values close to zero near high image gradients or edges.

## 4. Segmentation of Thermal Images

The general framework introduced in section 3 is applied to segment thermal images. The objective is to construct boundary elements of the given structure in the image.

We tested thermal images, from various applications such as medicine, defense and surveillance, with excellent results. We make no assumption about the object's shape, but use only three or four random points inside or around the interesting object as the initial points. Initial pixels locate the place where the evolution begins and provide some gradient information. The use of more initial pixels reduces the total segmentation time but has only a small effect on the final result.

### 4.1 Examples of Thermal Images

Segmenting thermal medical images is a means of identifying diseased tissues. Once diseased tissue has been segmented, it is useful to compare it with the normal tissue and see how it changes with pathology. For example, utilization of thermal imaging has been an effective method in the evaluation of vascular disease. Figure 2 shows a patient with vascular disease of the legs. The increased flow of blood through the vessel produces more heat, which is recordable with a thermal imaging procedure. Thermal imaging provides clues to the potential of developing

vascular disease, which may lead to stroke or cancer. An unsatisfied result is shown in Figure 2(f) with a general level set method proposed by [6]. The speed function without gradient directions cannot maintain the closed curve along the object boundary.

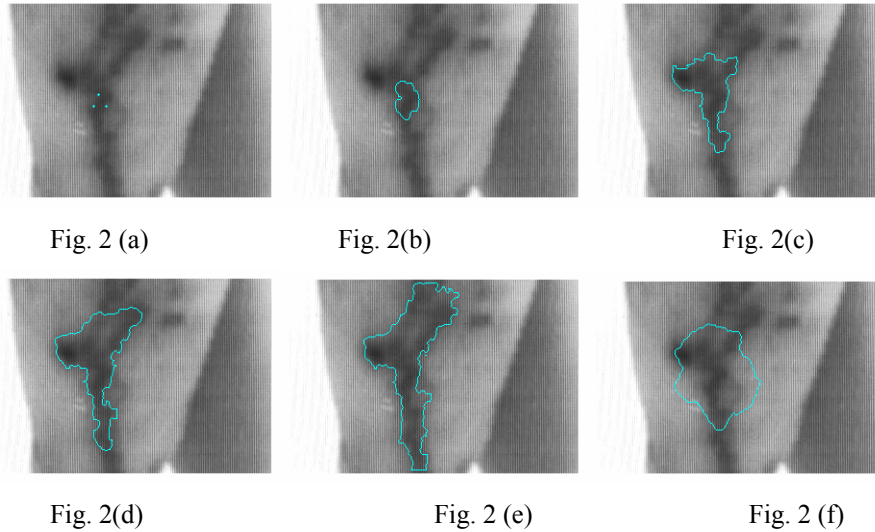


Fig. 2. (a) Three initial pixels. (b-d) Evolution of the boundary. (e) Final segmentation result. (f) Evolution without considering gradient directions.

Figure 3(a) shows a thermal image of a rat and four calibrating emitters. The four circles correspond to four emitters (only three are really apparent) at different temperatures, and the oblong shape is a live rat. The variability in shape adds to the segmentation challenge. The purpose of this experiment is to measure the thermal temperature of the rat. Figure 3(b) shows the boundaries of the rat and the four thermal emitters. The efficacy of this technique is really phenomenal, since using an edge operator on the image yields nowhere near a complete contour for the fourth emitter.

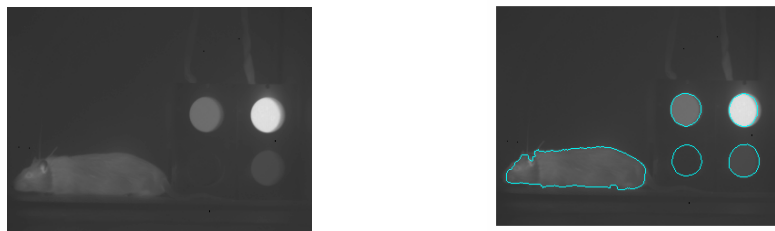


Fig. 3. (a) A thermal image of a rat and four calibrating emitters (only three are visible). (b) Segments of the rat and emitters.

Figures 4(a) shows an image taken from a sensor mounted on a helicopter. The result shows an example that our approach captures the corners. Figure 4(b) demonstrates how our

approach deals with noisy parts in the object. The curve flows around the noisy parts, because the curve always looks for the relatively homogenous region around its current position. After being isolated by the curve, the noisy parts are removed. This process implies that the curve ‘knows’ where the noisy parts are during its propagation. The result of our method is shown in Figure 4(d). The computed boundary captures the corners faithfully. In contrast, snake-based approaches tend to smooth the corners of solid objects. The boundary resulting from the snake proposed by Kass et al. [2] is shown in Figure 4(f), with the initial boundary shown in Figure 4(e). The final boundary produced by the snake approach looks too smooth because the first and the second derivatives are used as constraints in the classical snake [2].

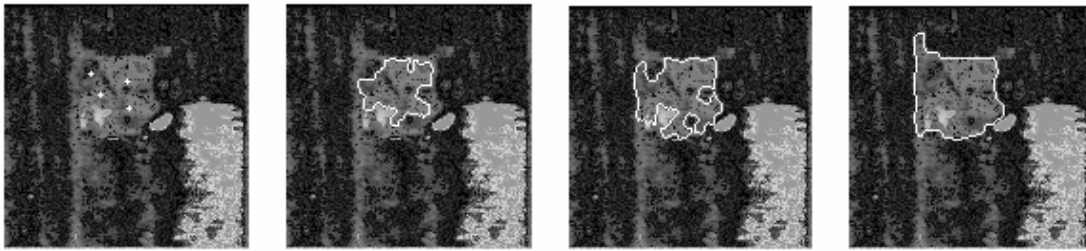


Fig. 4 (a)

Fig. 4 (b)

Fig. 4 (c)

Fig. 4 (d)

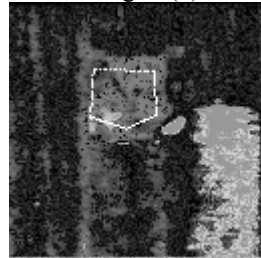


Fig. 4 (e)

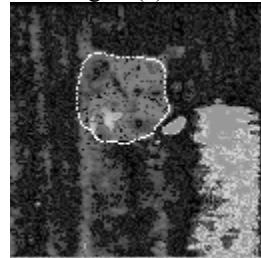


Fig. 4 (f)

## 4.2 Approach Comparison

The importance of the gradient direction in the speed function is emphasized in our paper. The introduction of the gradient direction as defined in our paper, overcomes the disadvantages in the general level set methods, which are summarized in [8].

a) The speed function may not turn out to be zero in multiple objects segmentation.

Fig.3 (a) shows a thermal image of a rat and four circular calibration emitters with very different intensities. The speed function of the brighter emitters can easily be reduced to zero while the dark emitters with low contrast from the background are likely to be missed by the evolving curve under the same model parameters. The active contour meets another problem in segmenting the rat and emitters, i.e. different shapes. Additional care is to be taken to set different



model parameters for the rat and emitters separately. In contrast, our proposed method segments all the five objects using the same parameters.

b) Embedding the object.

If one object has one or more objects located inside, the general level set method and the active contour will not capture all objects of interest. Our proposed curve flows around the noisy parts or the embedded objects, because the curve always looks for the relatively homogenous region around its current position. After being isolated by the curve, the noisy parts or embedded objects are located. This process implies that the curve ‘knows’ the noisy parts or embedded objects during its propagation. Fig.4(c) shows how the noisy parts or the embedded objects are located even though we remove them in Fig.4 (d).

c) Gaps in Boundaries.

Gaps in Boundaries are not a problem in the active contour model because the smoothing restriction and internal iterate values make the contour complete. However, they are the drawback of the level set method when applied to noisy images. The contour in the level set method is in an implicit form, which may simply leak through gaps.

## 5. Conclusion

In this paper we have presented a level set approach to segment thermal images. The edge map is introduced as the main component of the speed function. The edge map points toward the nearest boundary and its magnitude represents the total gradient energy in the half plane. The proposed approach uses both the edge direction and the gradient magnitude to overcome the problems resulting from weak edges. As shown in our experiments, our approach has several desirable features besides those of the general level set method. Good boundaries can be extracted from many kinds of thermal images with very few initial pixels inside or around the object; the final result is relatively independent of the initial guess; adding more initial pixels can reduce the total segmentation time; the parameters set in our experiments can work for thermal images from various applications; and the curve ‘knows’ where the isolated noisy parts are.

## References

- [1] J. Canny, "A Computational Approach to Edge Detection," *IEEE Trans. PAMI*, vol. 8, 679-698, Nov. 1986.
- [2] M. Kass, A. Witkin and D. Terzopoulos, "Snake: Active Contour Models," *Int. J. Comput. Vis.*, vol. 1, pp.321-331, 1987.
- [3] S. Osher and J. A. Sethian, "Front Propagation with Curvature-Dependent Speed: Algorithms Based on Hamilton-Jacobi formulation," *J. Computat. Phys.*, vol.79, pp.12-49, 1988.
- [4] G. Sapiro, *Geometric Partial Difference Equations and Image Analysis*, Cambridge University Press, Cambridge, UK, 2000.
- [5] V. Caselles, F. Catte and F. Dibos, "A Geometric Model for Active Contour in Image Processing," *Numerische Mathematik*, vol. 66, no. 1, pp. 1-31, 1993.
- [6] R. Malladi, J. A. Sethian and B. C. Vemuri, "Shape Modeling with Front Propagation: A Level Set Approach," *IEEE Trans. PAMI*, vol. 17, no. 2, pp. 158-175, Feb. 1995.
- [7] T. F. Chan and L. A. Vese, "Active Contour without Edges," *IEEE Trans. Image Processing*, vol. 10, no. 2, pp. 266-277, Feb. 2001.
- [8] J. S. Suri, K.Liu, S. Singh, S.N.Laxminarayan, X.Zeng and L.Reden, "Shape Recover Algorithms Using Level Sets in 2-D/3-D Medical Imagery: a State-of-the-Art Review," *IEEE Trans. Information Technology in Biomedicine*, vol.6, no.1, pp.8-28, March 2002.